Carbohydrate Polymers 102 (2014) 838–845

Contents lists available at ScienceDirect

Carbohydrate Polymers

journal homepage: www.elsevier.com/locate/carbpol

Physicochemical characterization of amphiphilic nanoparticles based on the novel starch–deoxycholic acid conjugates and self-aggregates

Jinlong Yang, Chunmei Gao, Shaoyu Lü, Xinjie Zhang, Chuanming Yu, Mingzhu Liu*

Key Laboratory of Nonferrous Metal Chemistry and Resources Utilization of Gansu Province, State Key Laboratory of Applied Organic Chemistry and Department of Chemistry, Lanzhou University, Lanzhou 730000, PR China

ARTICLE INFO

Article history:
Received 7 August 2013
Received in revised form 28 October 2013
Accepted 29 October 2013
Available online 7 November 2013

Keywords:
Starch
Deoxycholic acid
Self-aggregates
Nanoparticles

ABSTRACT

Novel amphiphilic polymers (starch–deoxycholic acid, St–DCA) were firstly synthesized on the basis of starch (St) as a hydrophilic segment and deoxycholic acid (DCA) as a hydrophobic segment. Hydrophobically modified starch contained 5.4–8.9 deoxycholic acid groups per 100 anhydroglucose units of starch. Self-aggregates of St–DCA conjugates were formed in the PBS media. Physicochemical characterizations of St–DCA conjugates were investigated. The mean sizes of self-aggregates decreased with the degree of substitution (DS) and pH increasing. Zeta potential indicated that nanoparticles were covered with negatively charged starch shells from −5.4 to −23 mV. TEM images demonstrated that nanoparticles were of spherical shape. The critical aggregation concentrations (cac) were dependent on the DS and pH in the range of 0.0185–0.0441 mg/mL. Thus, the study suggested that self-aggregated nanoparticles of St–DCA conjugates could have good pH-responsive and potential application in pharmaceutical and biomedical fields as the delivery of anti-tumor drugs.

1. Introduction

The various amphiphilic polymers consisting of hydrophilic and hydrophobic segments have been paid more and more attention as promising delivery systems of drugs and genes because of advantages such as their potential biotechnological, pharmaceutical applications, extending drug circulation time, enhancing its bioavailability and reducing the drug toxicity and side effects (Hu et al., 2008; Kataoka, Harada, & Nagasaki, 2001; Kim et al., 2005; Wang et al., 2011; Zhou et al., 2010). In the aqueous media, amphiphilic polymers form spontaneously micelles or self-aggregates, which are promoted *via* undergoing intra- or intermolecular association between hydrophobic segments because of the preference for the formation of free emergy-minimized structure (Akiyoshi, Deguchi, Moriguchi, Yamaguchi, & Sunamoto, 1993; Lee, Jo, Kwon, Kim, & Jeong, 1998a; Nagasaki, Yasugi, Yamamoto, Harada, & Kataoka, 2001; Wang et al., 2011). Considering that the formation of self-aggregation from amphiphilic polymers to resemble that of low molecular weight amphiphiles, these polymeric micelles or self-aggregates consist of the inner core of hydrophobic segments and the outer shell of hydrophilic segments, and core–shell structure has been recognized as a potential delivery carrier, because the inner core may serve as a microcontainer for various hydrophobic anticancer drugs (Kazunori, Glenn, Masayuki, Teruo, & Yasuhisa, 1993; Kim et al., 2000; Nakanishi et al., 2001; Wang et al., 2011). In the past decades, amphiphilic polymers have received much attention on the design and characterization of novel hydrophobically modified polymers due to their unique properties with respect to biotechnological and pharmaceutical applications (Du et al., 2006; Kuang et al., 2012; Lee, Jo, Kwon, Kim, & Jeong, 1998b; Xiong, Qi, & Yao, 2012).

The biocompatible and biodegradable properties of biomaterial carriers are two important factors in the development of nanoparticles drug delivery system (Zhou et al., 2010). Therefore, a number of nontoxic and biodegradable polymers have been used extensively as carrier materials such as poly (L-lysine), heparin, chitosan, dextran and pullulan (Abbasi et al., 2007; Jiang, Quan, Liao, & Wang, 2006; Li et al., 2009; Na, Lee, & Bae, 2007; Wang, Wang, Xiang, & Yao, 2010). Among the above polymers, natural polysaccharides such as chitosan, dextran, pullulan and curdlan, due to their outstanding advantages, have attracted much attention and been researched in the field of drug delivery systems (Hu et al., 2008; Liu, Jiao, Wang, Zhou, & Zhang, 2008). They have been hydrophobically modified with alkyl chains and bile acids to form micelles or self-aggregates in aqueous media (Wang et al., 2011). A great deal of studies has been reported to investigate and characterizes the properties of polysaccharide conjugates, especially developing their promising potential for biotechnology and medical application (Hu et al.,

* Corresponding author. Tel.: +86 931 8912387; fax: +86 931 8912582.
E-mail address: mzliu@lzu.edu.cn (M. Liu).

0144-8617/$ – see front matter © 2013 Elsevier Ltd. All rights reserved.
http://dx.doi.org/10.1016/j.carbpol.2013.10.081

2008). There have been many researches on hydrophobically modified chitosan and its derivatives in the recent years (Kwon et al., 2003; Park, Kwon, et al., 2004). However, there are few studies on self-aggregates of hydrophobically modified starch in the aqueous media.

Starch, next to chitosan and cellulose, is the most common polysaccharide and has a repeated structure of 1, 4-β-linked-D-glucose units, and is mainly used as the food additive. Starch has been known as a good candidate material for the preparation of nanocarriers, because it is biocompatible, biodegradable, non-immunogenicity and low toxicity. Starch and its derivatives are used extensively in drug delivery systems (Zhang, Zhang, et al., 2013). For example, hydrophobic starch derivatives, such as palmitoylated starch acetate (Tan, Xu, Li, Sun, & Wang, 2010) and propyl starch (Santander-Ortega et al., 2010), have been prepared to encapsulate anticancer drugs. In addition, the self-assembled micelles of hydrophobically modified starch have also been reported as a potential drug carrier, such as fatty acid modified hydroxyethyl starch and lipoic acid modified PEGylated starch (Besheer, Hause, Kressler, & Mäder, 2007; Zhang, Zhang, et al., 2013). Thus, in this study, starch was hydrophobically modified by deoxycholic acid to obtain self-aggregates in the PBS solution. Deoxycholic acid (DCA), a main component of bile acid, contains the hydrophilic moieties, such as the carboxyl group at the end of the branched side chain of carbon atoms and the hydroxyl groups at both 3α and 12α positions and the hydrophobic cyclopentenophenanthrene nucleus in its molecule (Wang et al., 2011). DCA is a main component of bile acid, which is the main product of cholesterol metabolism and biologically the most detergent-like molecule in the body (Kim et al., 2000; Lee et al., 1998a). Since DCA is known to form micelles in water because of its amphiphilicity, it plays an important role in the emulsification, solubilization, and absorption of cholesterol, fats, and liphophilic vitamins in the body (Enhsen, Kramer, & Wess, 1998). Thus, it is expected that the introduction of DCA into the starch could induce self-association to form self-aggregates.

In this study, starch was firstly hydrophobically modified by introducing DCA moieties to prepare the novel self-aggregated nanoparticles of starch–deoxycholic acid (St–DCA) conjugates by the coupling reaction between hydroxyl group of starch and carboxyl group of DCA. By varying the ratio of DCA, a series of St–DCA conjugates with different degree of substitution (DS) values were prepared. Herein, we investigated the effects of DS and pH on the formation of self-aggregates and the physicochemical characterization of St–DCA conjugates in detail.

2. Experimental

2.1. Materials

Soluble starch (Mw = 8.8 kDa) was purchased from Zhejiang Linghu Chemical Reagent Factory, chemical purity grade. 1-Ethyl-3-(3-dimethylaminopropyl) carbodiimide hydrochloride (EDC·HCl), *N*-hydroxysuccinimide (NHS) and deoxycholic acid (DCA) were purchased from Aladdin Reagent Inc. (Shanghai, China). Pyrene was purchased from Sigma–Aldrich. The other reagents were of analytical grade and used without further purification.

2.2. Synthesis of starch–deoxycholic acid (St–DCA) conjugates

Deoxycholic acid was grafted into the soluble starch by the coupling reaction between hydroxyl group of starch and carboxyl group of DCA as described by the literature (Dentini et al., 2001; Gao et al., 2008; Kim et al., 2013), and the reaction scheme was shown in Scheme 1A. Briefly, the soluble starch (0.162 g, 1 mmol) was dissolved in 15 mL DMSO under stirring at 45 °C. Different amounts of activated DCA (0.2–0.5 mol/mol sugar residues of starch) were added into the DMSO solution containing starch with the formation of ester linkages. To activate the carboxyl groups of DCA in the DMSO, equal amounts of EDC (1.2 equiv. DCA) and NHS (0.6 equiv. DCA, 15 min later) were added into DCA solution for 30 min at room temperature. The mixture was reacted under gentle stirring at 45 °C for 48 h. Then, the reactant mixture was cooled to room temperature and dialyzed against the excess amount of distilled water/methanol mixture (1:4, v/v) for 5 days using a dialysis tube (molecular cut off 7 kDa), and the distilled water/methanol mixture was exchanged at intervals of 8 h. Finally, the sample was followed by lyophilization to obtain St–DCA conjugates.

2.3. Characterization of the St–DCA conjugates

The chemical structure of St–DCA conjugates was confirmed using a Fourier transform infrared (FTIR) spectrometer (Nicolet 670 FTIR, USA) and ^{1}H NMR (Bruker Avance III 400, DMSO-d_6). Lyophilized St–DCA samples were pressed with KBr and scanned from 4000 to 400 cm^{-1} with a resolution of 4 cm^{-1}.

X-ray diffraction (XRD) spectrometry was obtained using XRD-6000 power diffractomer (Shimadzu, Japan). A Cu Kα radiation was used in range of 3–90° (2θ) at 40 kV and 40 mA.

2.4. Determination of DCA content and degree of substitution

The amount of DCA covalently bounded to starch was determined spectrophotometrically according to the procedure literatures (Gao et al., 2008; Nichifor & Carpov, 1999; Wang et al., 2011; Yuan, Li, & Yuan, 2006). Briefly, the polymer sample (4–10 mg) was accurately weighted and dissolved in 0.5 mL DMSO, then 0.5 mL acetic acid solution (60%) and 9.0 mL water/sulfuric acid (65/50, v/v) were subsequently added. The content of the sample solution was homogenized, heated at 70 °C for 30 min, and then cooled to room temperature. The UV (Lambda 35, Perkin Elmer, USA) absorbance of sample solution at 380 nm was measured against a blank containing the same components as the sample but without the polymer. Individual calibration curves of absorbance *verus* DCA concentrations were made. The DCA contents were determined according to calibration curves. The degree of substitution (DS, mol%, expressed as mole DCA/100 sugar residues of starch) was calculated according to the following formula.

$$\mathrm{DS} = \frac{16200 \times w}{392.57 \times (1 - w)}$$

where w is the content of the DCA determined from the corresponding calibration curve, 16,200 is 100 × Mw of glucose unit, and 392.57 is the molecular weight of the DCA residue.

2.5. Preparation of self-aggregated nanoparticles of St–DCA conjugates

The self-aggregated nanoparticles of St–DCA conjugates were prepared using a sonication method. The St–DCA conjugates (20 mg) were dissolved in 20 mL of phosphate buffered saline (PBS) solution with various pH under gentle shaking at 37 °C for 48 h, followed by sonication using a probe-type sonifier at 100 W for 10 min. The sonication was repeated three times to obtain optically transparent solution. To protect the solution from the heat build-up during sonication, the pulse function was used (pulse on, 5.0 s; pulse off, 2.0 s). The solution of self-aggregates was passed through a 0.45 μm filter (Millipore) and stored at room temperature.

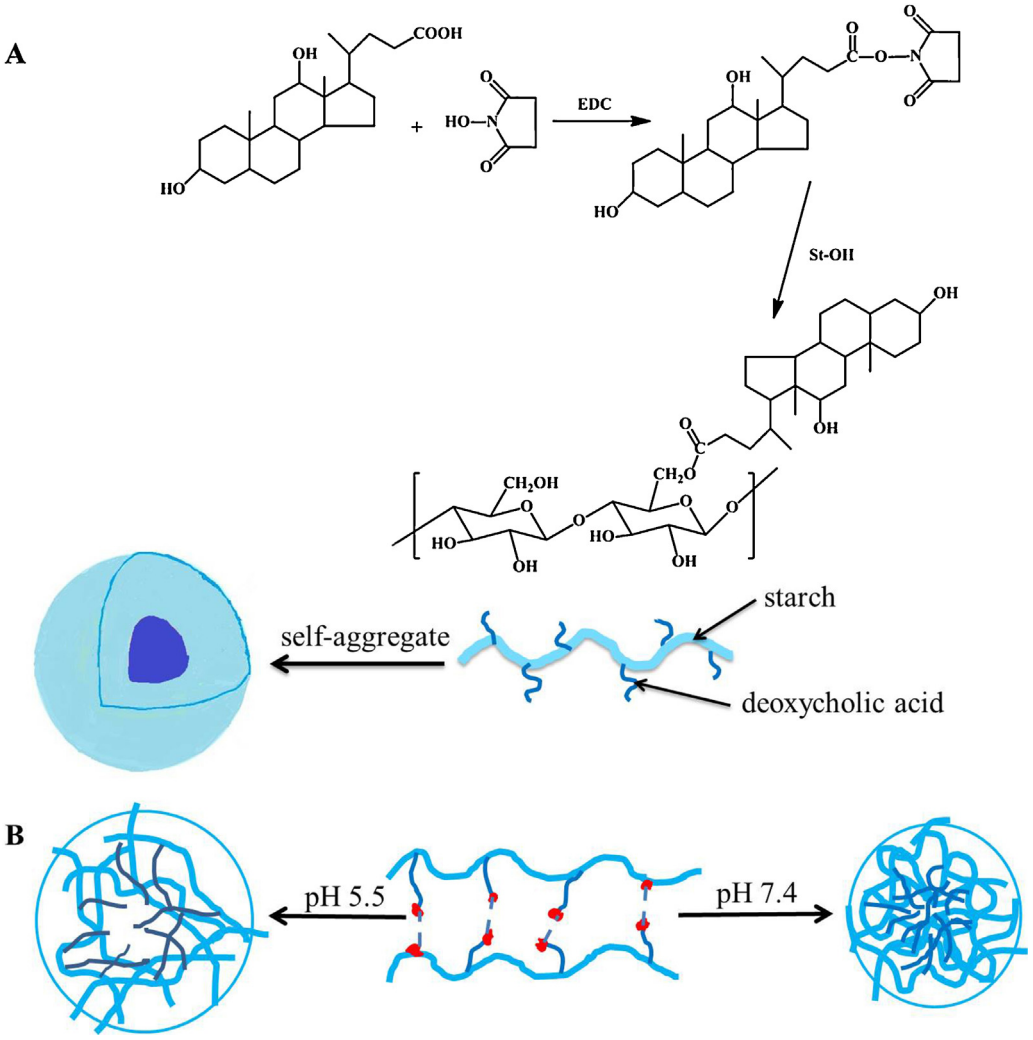

Scheme 1. (A) The synthesis schemes of St–DCA conjugates and schematic illustration of self-aggregated nanoparticles; (B) the schematic illustration of self-aggregated behaviors of St–DCA conjugates under different pH conditions.

2.6. Dynamic light scattering (DLS) and zeta potential measurements

The self-aggregated nanoparticles size was determined using DLS at room temperature on a 90Plus particle size analyzer (Brookhaven Instruments Corporation) at the 90° scattering angle. All sample solutions were filtered using disposable 0.45 μm Millipore filters prior to analysis at a concentration of 1.0 mg/mL.

The zeta potentials of self-aggregated nanoparticles were measured using a Zetasizer (Malvern Instruments Ltd, UK). The concentration of self-aggregates was kept constant at 1.0 mg/mL in various pH of PBS solution.

2.7. Morphology observation of self-aggregated nanoparticles

The morphology and size of self-aggregates were observed using transmission electron microscope (TEM) (Tecnai G^2 F20 S-Twin, FEI Company, USA). A drop of sample solution (1.0 mg/mL) was placed onto a 300-mesh copper grid coated with carbon. About 2 min after deposition, the grid was tapped with filter paper to remove surface water, followed by air-drying at room temperature and then observed at an acceleration voltage of 80 kV by TEM.

2.8. Fluorescence spectroscopy measurement

To investigate the fluorescence spectroscopy characteristics, the St–DCA conjugates suspension was prepared by the same procedure as the self-aggregated preparation. The potential of self-aggregated property and the critical aggregation concentration (cac) of St–DCA conjugates were estimated by the probe fluorescence technique in which pyrene was used as a hydrophobic probe. Briefly, a known amount of pyrene solutions (1 mL, 6×10^{-6} M) in acetone were added to a series of colorimetric tube (10 mL), and followed by evaporation to remove acetone. Then, the various concentrations (1×10^{-4} to 1.0 mg/mL) of St–DCA conjugate suspension were added to each colorimetric tube containing the pyrene residues with the final concentration of 6.0×10^{-7} mg/mL. The solutions were sonicated in an ultrasonic bath for 2 h to reach the solubilization equilibrium of pyrene between water phase and nanoaggregates overnight at room temperature. The excitation spectra of pyrene were recorded in the range of 300–350 nm using a fluorescence spectrophotometer (LS55, Perkin-Elmer, USA) at the emission wavelength (λ_{em}) of 390 nm and an integration time of 100 nm/min. The slit openings for excitation and emission were set at 15 and 15 nm, respectively.

3. Results and discussion

3.1. Synthesis and characterization of St–DCA conjugates

Hydrophobic deoxycholic acid with a rigid cyclopentenophenanthrene nucleus structure was selected to graft into

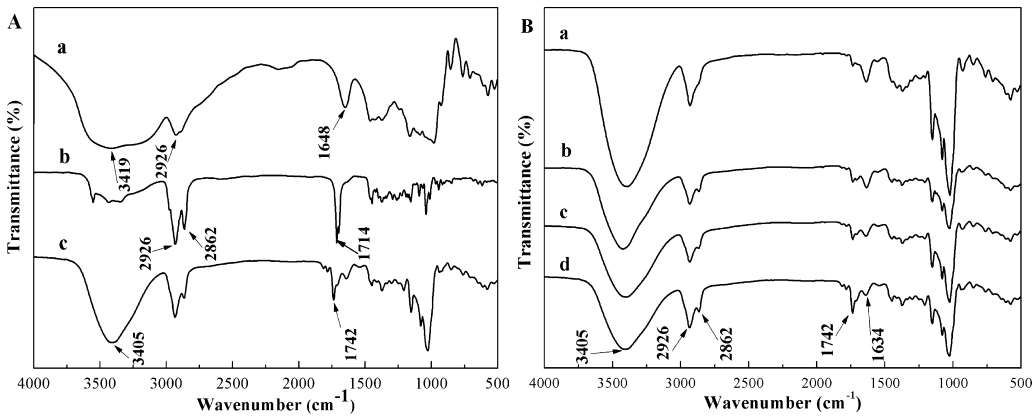

Fig. 1. (A) FTIR spectra of (a) starch, (b) DCA, and (c) St–DCA conjugate; (B) FTIR spectra of St–DCA conjugate derivatives: (a) St–$DCA_{5.4}$, (b) St–$DCA_{7.8}$, (c) St–$DCA_{8.0}$, and (d) St–$DCA_{8.9}$; 5.4, 7.8, 8.0, 8.9 are the degree of substitution (DS) of DCA.

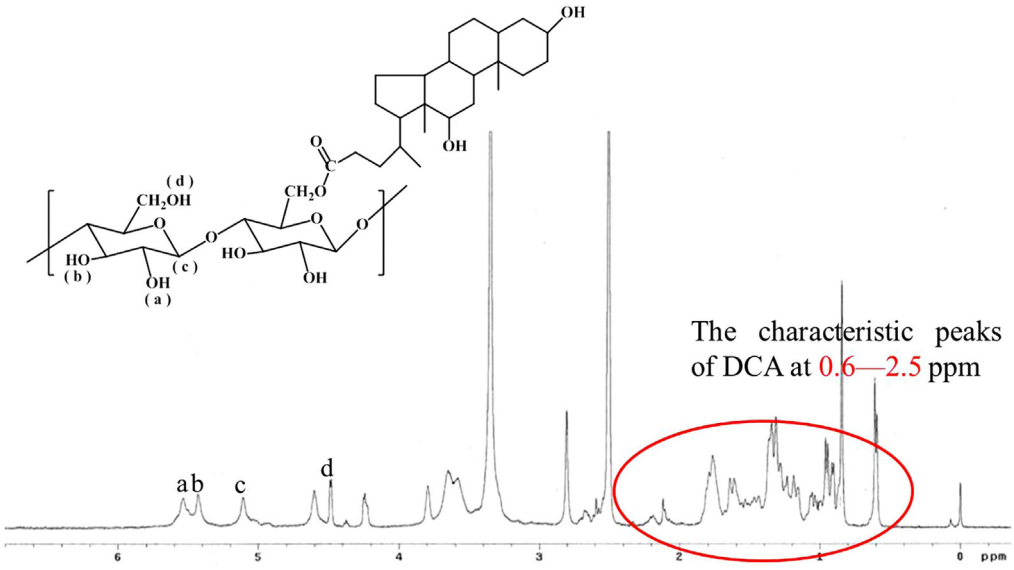

Fig. 2. ^{1}H NMR spectrum of St–DCA conjugates (DMSO-d_6).

starch. For the synthesis of St–DCA conjugates, deoxycholic acid was covalently attached to starch in the presence of "zero length" crosslinker of EDC and NHS reacted with a carboxyl group of the DCA to initially form an active ester intermediate, producing a novel kind of amphiphilic polymer. The various St–DCA conjugates with different DS of deoxycholic acid were firstly synthesized by controlling the feed ratio of DCA to starch. The synthesis procedure of St–DCA conjugates was illustrated in Scheme 1A. The DS of DCA was calculated through DCA content results. With the changed ratio of DCA to glucose units from 20 to 50%, the DS of DCA was changed from 5.4 to 8.9 with DCA contents in St–DCA conjugates ranged from 11.5 to 17.7% as shown in Table 1. The structure of St–DCA conjugates was confirmed by analysis of FTIR. The formation of ester linkage between DCA and starch was evidenced in the FTIR spectra in Fig. 1A, which showed the FTIR spectra of starch, DCA and St–DCA. The peak at 1648 cm^{-1} in the spectrum of starch (Fig. 1A(a)) was possibly a feature of water, and the bands at 3419 and 2926 cm^{-1} were characteristic of O—H and C—H stretches in the starch (Fang, Fowler, Sayers, & Williams, 2004). A significant shift at 1714 cm^{-1} was the carbonyl band of DCA units, and the characteristic peaks at 2926 and 2862 cm^{-1} (Fig. 1A(b)) were assigned to the stretching vibration of DCA (Cui et al., 2012). In comparison with the FTIR spectra of starch and DCA, the new absorption band at 1742 cm^{-1} (Fig. 1A(c)) was assigned to the carbonyl of ester bond of St–DCA, further confirming the formation of St–DCA conjugates. Fig. 1B showed the FTIR spectra of St–DCA conjugates with the different DS. It also showed that increasing of the feed ratio of DCA to starch (from 20 to 50%), the ester linkage peak at 1742 cm^{-1} became sharper and stronger, and the intensity of vibration of hydroxyl group at 3405 cm^{-1} became weaker, which indirectly indicated the increase of DS of DCA. The structure of St–DCA conjugates was also verified by ^{1}H NMR spectrum. Four peaks located between 4.5 and 5.6 ppm consisting of the C_2-O***H*** (**a**, 5.54 ppm), C_3-O***H*** (**b**, 5.43 ppm), C_1-***H***

Table 1
Properties of starch–deoxycholic acid (St–DCA) conjugates in PBS solution (pH = 7.4).

Sample	Feed ratio[a]	X^b (%)	DS[c]	d[d] (nm)	ζ[e] (mV)	cac[f](mg/mL)
St–$DCA_{5.4}$	0.2	11.5	5.4	247	−23	0.0383
St–$DCA_{7.8}$	0.3	16.0	7.8	223	−16.9	0.0342
St–$DCA_{8.0}$	0.4	16.3	8.0	198	−18.6	0.0269
St–$DCA_{8.9}$	0.5	17.7	8.9	182	−15.5	0.0185

[a] Mole ratio of DCA and sugar units of starch.
[b] Weight fraction of DCA.
[c] Degree of substitution of DCA per 100 glucose units of starch.
[d] Mean diameter measured by dynamic light scattering.
[e] The ζ-potential of St–DCA conjugated in PBS solution at 1 mg/mL.
[f] Critical aggregation concentration determined by fluorescence spectroscopy.

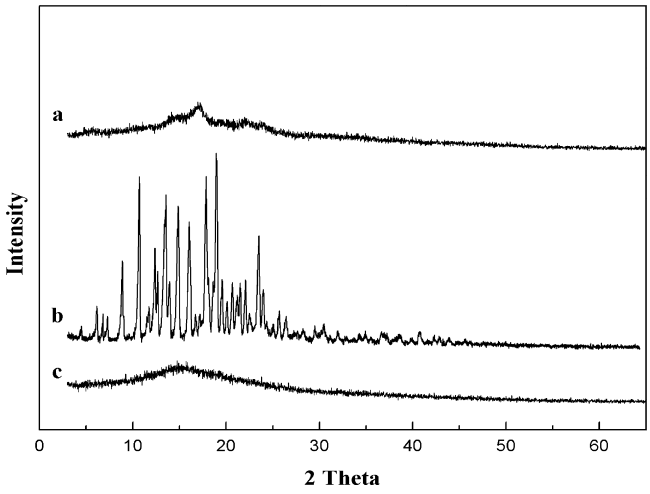

Fig. 3. XRD spectra of (a) starch, (b) DCA, and (c) St–DCA conjugate.

(**c**, 5.10 ppm) and C_6-O***H*** (**d**, 4.60 ppm) (Fig. 2) could be assigned to contribute to the hydroxyl groups from glucose unit of starch (Liu, Chaudhary, Yusa, & Tadé, 2011), which were also confirmed that the soluble starch were amylose. The characteristic peaks of DCA appearing at 0.6–2.5 ppm including 18-C$\boldsymbol{H}_3$ (0.60 ppm), 19-C$\boldsymbol{H}_3$ (0.90 ppm), 21-C$\boldsymbol{H}_3$ (0.99 ppm), and methylene–methine envelope (1–2.5 ppm) (Kim et al., 2005; Park, Kim, et al., 2004) in Fig. 2 were clearly observed, which could prove the presence of DCA in St–DCA conjugates.

3.2. Physical properties of St–DCA conjugates

To investigate the changes of the microstructure between starch and St–DCA conjugate, X-ray diffraction diagrams were showed in Fig. 3. The soluble starch had typical diffraction peaks at $2\theta = 17.3^\circ$, 22.0°, and 23.9°, which were assigned to the crystal form and were indicative of the B-type pattern (Cheetham & Tao, 1998). The diffraction curve of DCA showed eight typical crystal peaks at 2θ equals 10.7°, 13.3°, 13.9°, 14.7°, 16.0°, 17.8°, 18.9°, and 23.5°. In contrast of starch and DCA, St–DCA conjugates showed a broad diffraction peak at round $2\theta = 16.0^\circ$, and partial peaks disappeared and the intensity and location of peaks were changed obviously in the diffraction pattern of starch in St–DCA conjugates. The results indicated that the crystalline structure of starch had been completely disrupted after chemically modification, proving that DCA was coupled to starch successfully (Gao et al., 2008; Wang et al., 2011).

3.3. Self-aggregation of St–DCA conjugates

The amphiphilic St–DCA conjugates consisting of hydrophilic starch and hydrophobic deoxycholic acid could self-aggregate to form core–shell structure in the PBS solution with different pH values because of the contact between the hydrophobic side chains (Chiu et al., 2010). The hydrophobic DCA groups could aggregate spontaneously, which acted as physical cross-linkers between polymers (Xiong et al., 2012). St–DCA conjugates were dispersed in PBS solution at 37 °C for 48 h to obtain optical transparent solutions, followed by sonication to form self-aggregated nanoparticles. The brush-like structured core of nanoparticles was self-aggregated by hydrophobic effects of DCA, while the hydrophilic starch backbone comprised the shell of nanoparticles in Scheme 1A.

The size of self-aggregated nanoparticles of St–DCA conjugates with different DS in PBS solution (pH 7.4), which was determined by DLS. As shown in Table 1, the mean sizes of self-aggregated nanoparticles were in the range of 182–247 nm, depending on the DS values. The size of self-aggregates decreased as the DS increased, which indicated the formation of more compact hydrophobic cores, resulting in that the sizes were smaller, because the hydrophobic interaction was much stronger as the DCA contents in St–DCA conjugates increased (Wang et al., 2011). It was worthy to know that the size of self-aggregates based on St–DCA conjugates was obviously close to other amphiphilic polysaccharide polymers, such as deoxycholic acid modified chitosan (Hu et al., 2008; Lee et al., 1998a). The effects of pH on the self-aggregate nanoparticles of St–DCA conjugates were also important. The sizes of St–$DCA_{8.9}$ conjugates increased in PBS solution of different pH values varying from 7.4 to 5.5 (Table 2). The change could give a possible explain that the core–shell structure of nanoparticles was disrupted in the acidic conditions to agglomerate weakly resulting in large size and a little floccules, because the hydrogen-bond interactions between the hydroxyl groups of starch and DCA were greatly reduced under the acidic conditions, and the structure of self-aggregates became loose which led to the larger size as shown in Scheme 1B (Zhang, Shan, et al., 2013). Other possible season was that the electrostatic repulsion became weak between nanoparticles to form the larger aggregation of nanoparticles. Simultaneously, according to report of literatures (Chen et al., 2013; Cui et al., 2012), the pH-sensitivity of St–DCA conjugates was attributed to the introduced DCA ($pK_a = 6.58$) to form ester linkage, because the ester linkage was susceptible to the acidic environment to promote the partial hydrolysis of the ester linkage. In addition, the contents of obtained DCA as a result of hydrolysis further influenced the pH-responsive property of St–DCA conjugates. As a consequence, the partial hydrolysis under the acidic conditions could have an effect on core–shell structure of St–DCA conjugates to form loose structure. Furthermore, the hydrolysis degree increased with increased pH values in PBS solution, so that the size of St–DCA conjugates increased. But changes of particle sizes of St–DCA conjugates were only 40 nm (from 180 nm to 220 nm), mainly because the hydrolysis of St–DCA conjugates under acidic conditions was partial and incomplete.

Table 2
Properties of starch–deoxycholic acid (St–DCA) conjugate in PBS solutions of different pH.

Sample	pH	d[a] (nm)	ζ[b] (mV)	cac[c] (mg/mL)
St–$DCA_{8.9}$	5.5	225	−5.4	0.0441
	6.5	194	−10.2	0.0259
	7.4	182	−15.5	0.0185

[a] Mean diameter measured by dynamic light scattering.
[b] The ζ-potential of St–DCA conjugated in the various PBS solution at 1 mg/mL.
[c] Critical aggregation concentration determined by fluorescence spectroscopy.

The morphology of the self-aggregated nanoparticles was observed by transmission electron microscope (TEM). The images of St–$DCA_{5.4}$ (pH 7.4) and St–$DCA_{8.9}$ (pH 5.5 and 7.4) were chosen as samples in Fig. 4. The TEM results showed that the samples of these self-aggregated nanoparticles were spherical. But the size was smaller than the results determined by DLS measurement. It was ascribed to the solvent effect of different state of samples. It is well known that DLS provided the size for the particles swollen in the solution, whereas TEM images obtained the size at the dried state of the samples (Xiong et al., 2012). The images also showed that size of self-aggregated nanoparticles decreased with the DS increased, which was in a good agreement with the DLS results. However, these nanoparticles appeared a structural collapse when the pH was lowered from 7.4 to 5.5 as showed in Fig. 4c, because of pH-induced the self-aggregation of nanoparticles to make the microstructure destroyed under the acidic conditions, which resulted in their partial departure to make the self-aggregated nanoparticles decompose (Cui et al., 2012).

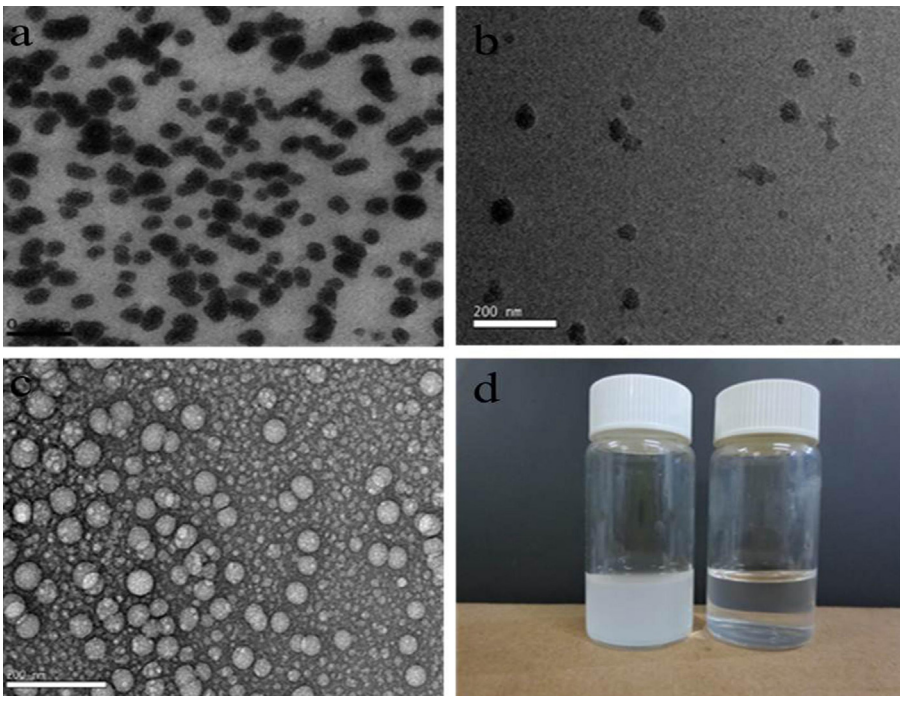

Fig. 4. TEM images of self-aggregated nanoparticles of St–DCA conjugates with different DS in different pH PBS solutions: (a) St–$DCA_{5.4}$ (pH 7.4), (b) St–$DCA_{8.9}$ (pH 7.4), (c) St–$DCA_{8.9}$ (pH 5.5). (d) A photograph of St–$DCA_{5.4}$ conjugate with before (left) and after (right) self-aggregation.

In Fig. 4d, the difference between the left vial and right vial was clearly found, which was mainly attributed to the solubility of starch. As we all know, the solubility is closely linked with temperature, and the solubility of starch is very poor in cold water. As a result, the amphiphilic St–DCA conjugates form self-aggregates consisting of the inner core of DCA and the outer shell of starch, so St–DCA conjugates looked like opaque solution in PBS solution of pH 7.4 (Fig. 4d, left), while the conjugates were at 37 °C for 48 h to obtain transparent solution (Fig. 4d, right) due to the increasing solubility of starch at 37 °C. Simultaneously, St–DCA conjugates were dispersed in PBS solution (pH 6.5 and 5.5) at 37 °C for 48 h to obtain transparent solution. However, the degree of transparency was weakly decreased under acidic condition, and it was in a small amount of turbidity in PBS solution of pH 5.5 (Fig. S1), which was attributed to hydrophobic molecule of DCA. Because the ester linkages were hydrolyzed partially in St–DCA conjugates to obtain free DCA under the acidic condition. Thus, it implied that the pH values had an effect on the self-aggregated process.

Supplementary material related to this article can be found, in the online version, at http://dx.doi.org/10.1016/j.carbpol.2013.10.081.

The zeta potential was very useful to predict the physical storage stability of the nanoparticles. If the nanoparticles had the higher zeta potential value, they would have the better stability (Wang et al., 2011). As shown in Tables 1 and 2, the zeta potential values of self-aggregated nanoparticles were negative ranged from −23 to −5.4 mV, which indicated that nanoparticles were covered with negatively charged starch, because starch had a negative charge with zeta potential of −10.3 mV in PBS solution (pH 7.4) (Minimol, Paul, & Sharma, 2013). And the absolute values of zeta potential of the self-aggregated nanoparticles were over 10.3 mV and gradually decreased as the DS increased in pH 7.4, which might be attributed to the electrolytes in PBS screen the negative charges in the starch backbone (Wang et al., 2011). However, their absolute value were below 10.3 mV in acidic conditions due to destroying the shell with negatively charged starch to make the charge decrease with the pH value decreasing, which was contributed to the slight protonation of hydroxyl groups under the acidic conditions. These results implied that the self-aggregated nanoparticles had a long term stability in physiological conditions, but the stability of nanoparticles was weaker in acidic conditions, which indicated that the nanoparticles were a promising carrier for drug release under the cancer cell environment.

3.4. Critical aggregation concentration of self-aggregated nanoparticles

The self-aggregation behavior of St–DCA conjugates in PBS solution media was determined using a probe fluorescence technique in the presence of pyrene, which is molecular fluorescence probe frequently used to measured the critical aggregation concentration (cac) of self-aggregates or micelles. The cac values are important evidences to prove the formation of self-aggregates (Zhou et al., 2010). Pyrene shows only small fluorescence intensity in a polar environment because of its poor solubility and self-quenching (Hu et al., 2008). With the formation of self-aggregated nanoparticles, the microenvironment of pyrene changed from hydrophilic to hydrophobic, it could preferably locate inside or close to the hydrophobic microenvironment of self-aggregates rather than the aqueous phase, resulting in different photophysical characteristics (Huh et al., 2000; Kim et al., 2005; Wilhelm et al., 1991; Zhou et al., 2010). The critical aggregation concentration (cac) was the threshold concentration of self-aggregated formation by intra- or intermolecular association. With the concentration increasing, the peaks of excitation spectra of pyrene in PBS solution were shifted from 326 to 329 nm, these results indicated that covalently coupled deoxycholic acids started to form hydrophobic domains in PBS solution. The cac could be determined from the intensity ratio (I_{329}/I_{326}) of the pyrene excitation spectra *versus* the logarithm of the St–DCA conjugates concentration, which was ranged from 1×10^{-4} to 1 mg/mL. The change of the intensity ratio was showed in Fig. 5. The cac values were estimated as the cross-point of two straight lines when extrapolating the intensity ratio (I_{329}/I_{326}) at low and high concentration regions, which were in the range of

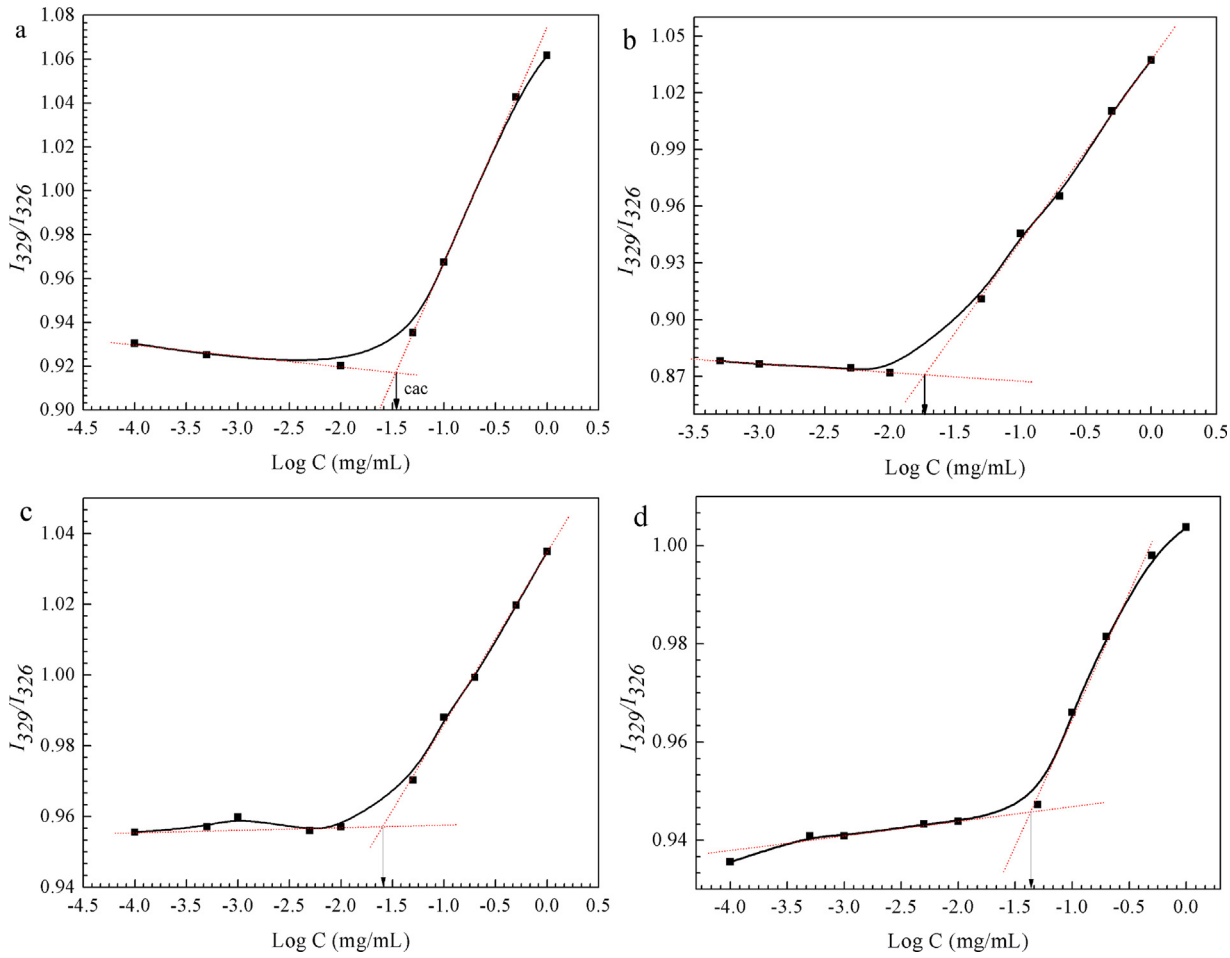

Fig. 5. Intensity ratios (I_{329}/I_{326}) from pyrene excitation spectra as a function of St–DCA conjugate concentration in PBS solution: (a) St–$DCA_{7.8}$ (pH 7.4), (b) St–$DCA_{8.9}$ (pH 7.4), (c) St–$DCA_{8.9}$ (pH 6.5), and (d) St–$DCA_{8.9}$ (pH 5.5).

0.0185–0.0383 mg/mL (Table 1). The cac values of the St–DCA conjugates decreased with the increase in the contents of hydrophobic DCA because of the enhanced hydrophobicity by introducing large amount of DCA moieties into the starch. And it was found that the cac values of St–DCA conjugates were even much lower than that of low molecular weight surfactants, such as 1.0 mg/mL for deoxycholic acid (Kratohvil, Hsu, & Kwok, 1986) and 2.3 mg/mL for sodium dodecyl sulfate (Rahman & Brown, 1983) in water. The values and its variation tendency were even similar and close to the cac values of deoxycholic acid-modified chitosan conjugates (0.013–0.045 mg/mL) (Lee et al., 1998b). The results indicated that the high molecular weight and hydrophobic nature of the starch backbone in St–DCA conjugates hampered significantly the effective association among hydrophobic DCA, and the St–DCA conjugates were a novel kind of amphiphilic polymers and could form the stable self-aggregates at low concentration in PBS solution media. It was evident that the cac values of self-aggregated nanoparticles could be controlled by the amount of DS (Na, Park, Kim, & Bae, 2000). Fig. 5 showed the intensity ratio from pyrene excitation spectra of St–DCA conjugates with different DS. When the DS increased from 5.4 to 8.9, their cac values were 0.0383, 0.0342, 0.0269 and 0.0185 mg/mL, respectively, which further confirmed that when the DS increased, the cac values could decrease. However, Fig. 5 and Table 2 showed that the cac values of St–$DCA_{8.9}$ conjugates were different in PBS solution with different pH, and the cac values decreased with increasing pH due to the effective hydrophobic interaction enhancing. As shown in Scheme 1B, when the self-aggregates of St–$DCA_{8.9}$ conjugates were in the neutral condition, the hydrogen-bond interactions between the hydroxyl groups of starch and DCA were enhanced to make hydrophobicity improve, and self-aggregates became compact simultaneously to obtain the smaller cac values. On the contrary, the hydrogen-bond interactions became reduced and the ester linkages in St–DCA conjugates were hydrolyzed partially under the acidic condition, which led to the loose self-aggregates (Zhang, Shan, et al., 2013).

4. Conclusions

A novel kind of amphiphilic polymers, hydrophobically modified starch by deoxycholic acid (St–DCA), was prepared and characterized by FTIR, ^{1}H NMR and XRD. The various physicochemical properties of self-aggregated nanoparticles with different DS and pH were investigated. The mean sizes of self-aggregates of St–DCA conjugates were in the range of 182–247 nm, and the critical aggregation concentrations (cac) of St–DCA conjugates were in the range of 0.0185–0.0447 mg/mL, which indicated that the mean sizes and cac values depended on the DS and pH values. The zeta potentials of self-aggregated nanoparticles were negative. The TEM images showed that self-aggregated nanoparticles were spherical. The self-aggregated nanoparticles of St–DCA conjugates had a good pH-responsive. The results of physicochemical properties could suggest the potential applications of the novel self-aggregated nanoparticles in the pharmaceutical and biomedical fields, especially, in the delivery of bioactive agents such as anti-tumor drugs.

Acknowledgment

The authors acknowledge gratefully the financial support of the National Natural Science Foundation of China (Grant no. 51273086).

References

Abbasi, M., Uludağ, H., Incani, V., Olson, C., Lin, X., Clements, B. A., et al. (2007). Palmitic acid-modified poly-L-lysine for non-viral delivery of plasmid DNA to skin fibroblasts. *Biomacromolecules*, *8*(4), 1059–1063.

Akiyoshi, K., Deguchi, S., Moriguchi, N., Yamaguchi, S., & Sunamoto, J. (1993). Self-aggregates of hydrophobized polysaccharides in water. Formation and characteristics of nanoparticles. *Macromolecules*, *26*(12), 3062–3068.

Besheer, A., Hause, G., Kressler, J., & Mäder, K. (2007). Hydrophobically modified hydroxyethyl starch: Synthesis, characterization, and aqueous self-assembly into nano-sized polymeric micelles and vesicles. *Biomacromolecules*, *8*(2), 359–367.

Cheetham, N. W. H., & Tao, L. (1998). Variation in crystalline type with amylose content in maize starch granules: An X-ray powder diffraction study. *Carbohydrate Polymers*, *36*(4), 277–284.

Chen, D., Song, P., Jiang, F., Meng, X., Sui, W., Shu, C., et al. (2013). pH-responsive mechanism of a deoxycholic acid and folate comodified chitosan micelle under cancerous environment. *Journal of Physical Chemistry B*, *117*(5), 1261–1268.

Chiu, Y.-L., Ho, Y.-C., Chen, Y.-M., Peng, S.-F., Ke, C.-J., Chen, K.-J., et al. (2010). The characteristics, cellular uptake and intracellular trafficking of nanoparticles made of hydrophobically-modified chitosan. *Journal of Controlled Release*, *146*(1), 152–159.

Cui, W., Lu, X., Cui, K., Niu, L., Wei, Y., & Lu, Q. (2012). Dual-responsive controlled drug delivery based on ionically assembled nanoparticles. *Langmuir*, *28*(25), 9413–9420.

Dentini, M., Desideri, P., Crescenzi, V., Yuguchi, Y., Urakawa, H., & Kajiwara, K. (2001). Synthesis and physicochemical characterization of gellan gels. *Macromolecules*, *34*(5), 1449–1453.

Du, J.-Z., Chen, D.-P., Wang, Y.-C., Xiao, C.-S., Lu, Y.-J., Wang, J., et al. (2006). Synthesis and micellization of amphiphilic brush–coil block copolymer based on poly(ε-caprolactone) and PEGylated polyphosphoester. *Biomacromolecules*, *7*(6), 1898–1903.

Enhsen, A., Kramer, W., & Wess, G. (1998). Bile acids in drug discovery. *Drug Discovery Today*, *3*(9), 409–418.

Fang, J. M., Fowler, P. A., Sayers, C., & Williams, P. A. (2004). The chemical modification of a range of starches under aqueous reaction conditions. *Carbohydrate Polymers*, *55*(3), 283–289.

Gao, F.-P., Zhang, H.-Z., Liu, L.-R., Wang, Y.-S., Jiang, Q., Yang, X.-D., et al. (2008). Preparation and physicochemical characteristics of self-assembled nanoparticles of deoxycholic acid modified-carboxymethyl curdlan conjugates. *Carbohydrate Polymers*, *71*(4), 606–613.

Hu, Y., He, X., Lei, L., Liang, S., Qiu, G., & Hu, X. (2008). Preparation and characterization of self-assembled nanoparticles of the novel carboxymethyl pachyman–deoxycholic acid conjugates. *Carbohydrate Polymers*, *74*(2), 220–227.

Huh, K. M., Lee, K. Y., Kwon, I. C., Kim, Y.-H., Kim, C., & Jeong, S. Y. (2000). Synthesis of triarmed poly(ethylene oxide)–deoxycholic acid conjugate and its micellar characteristics. *Langmuir*, *16*(26), 10566–10568.

Jiang, G.-B., Quan, D., Liao, K., & Wang, H. (2006). Novel polymer micelles prepared from chitosan grafted hydrophobic palmitoyl groups for drug delivery. *Molecular Pharmaceutics*, *3*(2), 152–160.

Kataoka, K., Harada, A., & Nagasaki, Y. (2001). Block copolymer micelles for drug delivery: Design, characterization and biological significance. *Advanced Drug Delivery Reviews*, *47*(1), 113–131.

Kazunori, K., Glenn, S. K., Masayuki, Y., Teruo, O., & Yasuhisa, S. (1993). Block copolymer micelles as vehicles for drug delivery. *Journal of Controlled Release*, *24*(1–3), 119–132.

Kim, C., Lee, S. C., Kang, S. W., Kwon, I. C., Kim, Y.-H., & Jeong, S. Y. (2000). Synthesis and the micellar characteristics of poly(ethylene oxide)–deoxycholic acid conjugates. *Langmuir*, *16*(11), 4792–4797.

Kim, H., Park, S. S., Seo, J., Ha, C.-S., Moon, C., & Kim, Y. (2013). Stable protein device platform based on pyridine dicarboxylic acid-bound cubic-nanostructured mesoporous titania films. *ACS Applied Materials & Interfaces*, *5*(15), 6873–6878.

Kim, K., Kwon, S., Park, J. H., Chung, H., Jeong, S. Y., Kwon, I. C., et al. (2005). Physicochemical characterizations of self-assembled nanoparticles of glycol chitosan–deoxycholic acid conjugates. *Biomacromolecules*, *6*(2), 1154–1158.

Kratohvil, J. P., Hsu, W. P., & Kwok, D. I. (1986). How large are the micelles of di-α-hydroxy bile salts at the critical micellization concentrations in aqueous electrolyte solutions? Results for sodium taurodeoxycholate and sodium deoxycholate. *Langmuir*, *2*(2), 256–258.

Kuang, H., Wu, S., Xie, Z., Meng, F., Jing, X., & Huang, Y. (2012). Biodegradable amphiphilic copolymer containing nucleobase: Synthesis, self-assembly in aqueous solutions, and potential use in controlled drug delivery. *Biomacromolecules*, *13*(9), 3004–3012.

Kwon, S., Park, J. H., Chung, H., Kwon, I. C., Jeong, S. Y., & Kim, I.-S. (2003). Physicochemical characteristics of self-assembled nanoparticles based on glycol chitosan bearing 5β-cholanic acid. *Langmuir*, *19*(24), 10188–10193.

Lee, K. Y., Jo, W. H., Kwon, I. C., Kim, Y.-H., & Jeong, S. Y. (1998a). Physicochemical characteristics of self-aggregates of hydrophobically modified chitosans. *Langmuir*, *14*(9), 2329–2332.

Lee, K. Y., Jo, W. H., Kwon, I. C., Kim, Y.-H., & Jeong, S. Y. (1998b). Structural determination and interior polarity of self-aggregates prepared from deoxycholic acid-modified chitosan in water. *Macromolecules*, *31*(2), 378–383.

Li, Y.-L., Zhu, L., Liu, Z., Cheng, R., Meng, F., Cui, J.-H., et al. (2009). Reversibly stabilized multifunctional dextran nanoparticles efficiently deliver doxorubicin into the nuclei of cancer cells. *Angewandte Chemie International Edition*, *48*(52), 9914–9918.

Liu, H., Chaudhary, D., Yusa, S.-i., & Tadé, M. O. (2011). Glycerol/starch/Na^+-montmorillonite nanocomposites: A XRD, FTIR, DSC and 1H NMR study. *Carbohydrate Polymers*, *83*(4), 1591–1597.

Liu, Z., Jiao, Y., Wang, Y., Zhou, C., & Zhang, Z. (2008). Polysaccharides-based nanoparticles as drug delivery systems. *Advanced Drug Delivery Reviews*, *60*(15), 1650–1662.

Minimol, P. F., Paul, W., & Sharma, C. P. (2013). PEGylated starch acetate nanoparticles and its potential use for oral insulin delivery. *Carbohydrate Polymers*, *95*(1), 1–8.

Na, K., Lee, E. S., & Bae, Y. H. (2007). Self-organized nanogels responding to tumor extracellular pH: pH-dependent drug release and in vitro cytotoxicity against MCF-7 cells. *Bioconjugate Chemistry*, *18*(5), 1568–1574.

Na, K., Park, K.-H., Kim, S. W., & Bae, Y. H. (2000). Self-assembled hydrogel nanoparticles from curdlan derivatives: Characterization, anti-cancer drug release and interaction with a hepatoma cell line (HepG2). *Journal of Controlled Release*, *69*(2), 225–236.

Nagasaki, Y., Yasugi, K., Yamamoto, Y., Harada, A., & Kataoka, K. (2001). Sugar-installed block copolymer micelles: Their preparation and specific interaction with lectin molecules. *Biomacromolecules*, *2*(4), 1067–1070.

Nakanishi, T., Fukushima, S., Okamoto, K., Suzuki, M., Matsumura, Y., Yokoyama, M., et al. (2001). Development of the polymer micelle carrier system for doxorubicin. *Journal of Controlled Release*, *74*(1–3), 295–302.

Nichifor, M., & Carpov, A. (1999). Bile acids covalently bound to polysaccharides 1. Esters of bile acids with dextran. *European Polymer Journal*, *35*(12), 2125–2129.

Park, J. H., Kwon, S., Nam, J.-O., Park, R.-W., Chung, H., Seo, S. B., et al. (2004). Self-assembled nanoparticles based on glycol chitosan bearing 5β-cholanic acid for RGD peptide delivery. *Journal of Controlled Release*, *95*(3), 579–588.

Park, K., Kim, K., Kwon, I. C., Kim, S. K., Lee, S., Lee, D. Y., et al. (2004). Preparation and characterization of self-assembled nanoparticles of heparin–deoxycholic acid conjugates. *Langmuir*, *20*(26), 11726–11731.

Rahman, A., & Brown, C. W. (1983). Effect of pH on the critical micelle concentration of sodium dodecyl sulphate. *Journal of Applied Polymer Science*, *28*(4), 1331–1334.

Santander-Ortega, M. J., Stauner, T., Loretz, B., Ortega-Vinuesa, J. L., Bastos-González, D., Wenz, G., et al. (2010). Nanoparticles made from novel starch derivatives for transdermal drug delivery. *Journal of Controlled Release*, *141*(1), 85–92.

Tan, Y., Xu, K., Li, Y., Sun, S., & Wang, P. (2010). A robust route to fabricate starch esters vesicles. *Chemical Communications*, *46*(25), 4523–4525.

Wang, F., Zhang, D., Duan, C., Jia, L., Feng, F., Liu, Y., et al. (2011). Preparation and characterizations of a novel deoxycholic acid–O-carboxymethylated chitosan–folic acid conjugates and self-aggregates. *Carbohydrate Polymers*, *84*(3), 1192–1200.

Wang, Y., Wang, Y., Xiang, J., & Yao, K. (2010). Target-specific cellular uptake of taxol-loaded heparin-PEG-folate nanoparticles. *Biomacromolecules*, *11*(12), 3531–3538.

Wilhelm, M., Zhao, C. L., Wang, Y., Xu, R., Winnik, M. A., Mura, J. L., et al. (1991). Poly(styrene-ethylene oxide) block copolymer micelle formation in water: A fluorescence probe study. *Macromolecules*, *24*(5), 1033–1040.

Xiong, Y., Qi, J., & Yao, P. (2012). Amphiphilic cholic-acid-modified dextran sulfate and its application for the controlled delivery of superoxide dismutase. *Macromolecular Bioscience*, *12*(4), 515–524.

Yuan, X.-b., Li, H., & Yuan, Y.-b. (2006). Preparation of cholesterol-modified chitosan self-aggregated nanoparticles for delivery of drugs to ocular surface. *Carbohydrate Polymers*, *65*(3), 337–345.

Zhang, A., Zhang, Z., Shi, F., Ding, J., Xiao, C., Zhuang, X., et al. (2013). Disulfide crosslinked PEGylated starch micelles as efficient intracellular drug delivery platforms. *Soft Matter*, *9*(7), 2224–2233.

Zhang, Z., Shan, H., Chen, L., He, C., Zhuang, X., & Chen, X. (2013). Synthesis of pH-responsive starch nanoparticles grafted poly (L-glutamic acid) for insulin controlled release. *European Polymer Journal*, *49*(8), 2082–2091.

Zhou, H., Yu, W., Guo, X., Liu, X., Li, N., Zhang, Y., et al. (2010). Synthesis and characterization of amphiphilic glycidol–chitosan–deoxycholic acid nanoparticles as a drug carrier for doxorubicin. *Biomacromolecules*, *11*(12), 3480–3486.